

# Modulation of spin-orbit coupled Bose-Einstein condensates: analytical characterization of acceleration-induced transitions between energy bands

J.M. Gomez Llorente and J. Plata

*Departamento de Física, Universidad de La Laguna,*

*La Laguna E38204, Tenerife, Spain.*

## Abstract

The effects of modulating spin-orbit coupled Bose-Einstein condensates are analytically studied. A sinusoidal driving of the coupling amplitude is shown to induce significant changes in the energy bands and in the associated spin-momentum locking. Moreover, in agreement with recent experimental results, gravitational acceleration of the modulated system is found to generate transitions between the modified energy bands. The applicability of the Landau-Zener (LZ) model to the understanding of the experimental findings is rigorously traced. Through a sequence of unitary transformations and the reduction to the spin space, the modulated Hamiltonian, with the gravitational potential incorporated, is shown to correspond to an extended version of the LZ scenario. The generalization of the basic LZ model takes place along two lines. First, the dimensionality is enlarged to combine the description of the external dynamics with the internal-state characterization. Second, the model is extended to incorporate two avoided crossings emerging from the changes induced in the energy bands by the modulation. Our approach allows a first-principle derivation of the effective model-system parameters. The obtained analytical results provide elements to control the transitions.

## I. INTRODUCTION

The realization of Bose-Einstein condensates (BECs) with synthetic spin-orbit coupling (SOC) [1] has opened an active field of research where the progress in theory and experiments is continuous [2]. The implementation of diverse variations of the basic scenario have led to significant advances. Particularly interesting are the extensions to different spin values [3] or to fermionic systems [4, 5], the study of excitations [6–13] with the analysis of dynamical instability [14, 15], or the incorporation of optical lattices [16] and the research on superfluidity [17, 18]. The variety of emerging physical effects, along with the possibility of controlling the experimental conditions, allows regarding those systems as a testing ground for the predictions of fundamental theories. In this sense, it is worth mentioning the effort made in exploring the potential appearance of novel states of matter, like nontrivial superfluids or topological insulators [1, 19–21]. Crucial to the development of the field is the implementation of methods to control the dynamics. Here, we focus on recent experiments, realized in the *standard* Raman-laser setup, which have uncovered the possibility of implementing controlled variations of basic properties of the system through the modulation of the Raman-coupling amplitude [22]. Specifically, a sinusoidal modulation of the coupling amplitude was found to induce nontrivial changes in the energy bands and in the associated spin polarization. Moreover, gravitational acceleration of the modulated system was shown to generate transitions between the modified energy bands. An approach based on the application of the Floquet formalism [23] was set up to explain the findings. However, because of the complexity of the description, no analytical insight was extracted from the complete Floquet picture. In fact, it was in an operative reduction to a two-level system with adjustable parameters where a satisfactory emulation of the experimental results was produced. In particular, some general aspects of the transitions were explained using an effective Landau-Zener (LZ) model [24, 25] with two avoided crossings. The realization of Stueckelberg interferometry [26] using the found structure of connected bands served to test the theoretical framework: the achieved emulation of the experimental output can be considered as a proof of consistency. Although the compact character of the employed model allows envisaging the control of the analyzed effects, the need of using adjustable parameters seems to be a serious limiting factor. In our work, we go further along the lines depicted in those preliminary analyses by presenting an approximate analytical description of the sys-

tem response to the modulation. In our framework, set up from first principles and with no adjustable parameters, the applicability of a generalized LZ model will be rigorously shown. Our approach generalizes the methodology used in previous work where related problems were tackled. Namely, in [27], the use of a high-frequency driving to modify in a controlled way the SOC magnitude, and, in turn, the ground state, was experimentally evaluated. The reduced efficiency of the method in particular spectral ranges was conjectured to be due to heating. Identifying the heating mechanism was the objective of the theoretical study of [28]. There, a perturbative scheme was found to provide the appropriate tools to explain the experimental findings and to improve the performance of the proposed technique. Additional related research was presented in [29]. There, experimental work on an unmodulated spin-orbit-coupled Bose-Einstein condensate (SOBEC) uncovered the existence of inter-band transitions induced by the acceleration of the system. In early analyses of those experiments, an operative LZ model was applied to the characterization of the transition probabilities [29],[30]. Subsequently, in [31], an approximate analytical description of the two, gravitational and harmonic, acceleration schemes implemented in practice was provided. The scenario considered in those previous studies must be generalized to deal with the system implemented in [22]: first, it is necessary to evaluate the combined effect of modulation and acceleration on a SOBEC; second, it is essential going beyond the perturbative regime considered in [28]. Following those requirements, we present here a compact description of the dynamics, where the mechanisms responsible for the observed effects can be identified. Our approach is built up through a sequence of unitary transformations. We start by transferring the modulation of the Raman-coupling amplitude to multiple driving terms in the Hamiltonian. By pondering the relative importance of those terms, we will be able to single out the components, and, in turn, the mechanisms, that generate the changes detected in the system properties. The procedure ends with the derivation of a compact two-level Hamiltonian with a structure similar to that of the model phenomenologically introduced in [22], and, with effective parameters directly connected with the system characteristics. In this approach, the observed energy bands are reproduced, and, from the associated dressed states, the *evolution* of the spin polarization along the bands is analytically emulated. Additionally, a generalized LZ model with two avoided crossings and the energy mismatch linearly varying because of gravity is shown to be applicable to the observed acceleration-induced transitions. Hence, our study supports and generalizes the effective model employed in [22].

The analytical character of the whole picture and the established connection between the effective-model parameters and the system characteristics provide us with some useful clues to implement strategies of control.

The outline of the paper is as follows. In Sec. II, the model system and the basic elements of our methodology are introduced. In Sec. III, we derive an effective undriven system which is shown to account for the basic characteristics of the dynamics. Sec. IV is dedicated to the description of the inter-band transitions induced by gravitational acceleration. A generalized LZ model appropriate to describe those transitions is derived and the effective parameters of the model are identified. Finally, in Sec. V, a discussion of the implications and potential extension of the study is presented.

## II. MODULATED SPIN-ORBIT COUPLING

### The model system

We focus on the realization of synthetic SOC in a one-dimensional BEC reported in [22]. The coupling of the external linear momentum of the atoms  $\mathbf{p}$  to an effective “spin”, i.e., to a two-level internal system formed by hyperfine states, was achieved through the use of two orthogonally polarized Raman lasers with different propagation directions and frequencies. Specifically, coupling dependent on the atom external momentum was implemented between the three Zeeman-split states  $|F, m_F\rangle$  of the hyperfine  $F = 1$  ground-state manifold of  $Rb^{87}$ . Moreover, the detuning due to the quadratic Zeeman shift was used to reduce the dynamics to the two levels associated to  $m_F = 0, -1$ . The corresponding states will be denoted as  $|1, m_F = 0\rangle \equiv |\downarrow\rangle$  and  $|1, m_F = 1\rangle \equiv |\uparrow\rangle$ . An essential component of the effective SOC created in [22] was the modulation of the Raman-coupling amplitude  $\Omega_R(t)$ . The characterization of the effects resulting from that modulation constitutes the central objective of the present study. The system is modeled by the (driven) Hamiltonian

$$H_{SOC}(t) = \frac{P_y^2}{2m} + E_r \hat{1} + \frac{\hbar\Omega_R(t)}{2} \hat{\sigma}_x + \left( \frac{\hbar\delta}{2} + \frac{\alpha P_y}{\hbar} \right) \hat{\sigma}_z, \quad (1)$$

where  $m$  denotes the atomic mass,  $P_y$  stands for the momentum operator, and  $\sigma_i$  ( $i = x, y, z$ ) are the Pauli matrices corresponding to the *pseudospin*, i.e., to the considered effective two-level system. The rest of parameters refer to the laser characteristics:  $\alpha = 2E_r/k_r$  is the

strength of the realized SOC;  $E_r = \hbar^2 k_r^2 / 2m$  and  $k_r = 2\pi \sin(\theta/2) / \lambda$  are, respectively, the recoil energy and momentum;  $\lambda$  is the reference laser wavelength, and,  $\theta$  is the angle between the directions of the Raman lasers, which, here, is fixed to  $\theta = \pi/2$ . Moreover,  $\delta$  denotes an adjustable detuning. In the considered experimental realization, a sinusoidal modulation of the Raman-coupling amplitude  $\Omega_R$ , with amplitude  $\Omega_M$  and frequency  $\omega_M$ , was implemented. Specifically,  $\Omega_R$ , with mean value  $\Omega_0$ , was varied according to

$$\Omega_R(t) = \Omega_0 + \Omega_M \cos(\omega_M t). \quad (2)$$

No harmonic confinement is considered. The relevance of this restriction will be discussed further on.

Before dealing with the effect of the modulation of the Raman amplitude, it is pertinent to review some general characteristics of the undriven scenario, i.e., of the system corresponding to take  $\Omega_M = 0$  in Eq. (2). In former research [1, 29], general aspects of that system were analyzed using a single-particle description as a first-stage approach. In particular, some properties of the energy bands were described. From that work, one can extract the following general considerations to take into account in our study:

First, since  $P_y$  is a constant of the motion, it is appropriate to use the basis  $\{|p_y\rangle \otimes |\chi\rangle\}$ , where  $|p_y\rangle$  denotes a momentum state and  $|\chi\rangle$  stands for a spin state. Then, the Hamiltonian can be reduced to the spin space by simply replacing the operator  $P_y$  by  $\hbar q$  in Eq. (1). ( $q$  is the quasi-momentum in the coupling direction,  $p_y = \hbar q$ ). Hence, it is straightforwardly shown that the system presents the lower and upper (undriven) energy bands,  $E_-^{(ud)}$  and  $E_+^{(ud)}$ , given by

$$E_{\pm}^{(ud)}(q) = \frac{\hbar^2 q^2}{2m} + E_r \pm \sqrt{\left(\frac{\hbar \Omega_0}{2}\right)^2 + \left(\frac{\hbar \delta}{2} + \alpha q\right)^2}. \quad (3)$$

Moreover, since the bands correspond to eigenvalues of the reduced Hamiltonian, no transitions between them are predicted to occur in this scheme. Indeed, the bands reflect the existence of locking between the momentum and the spin state: each quasi-momentum value  $q$  is attached to a particular pair of eigenvalues,  $E_-^{(ud)}(q)$  and  $E_+^{(ud)}(q)$ , and, in turn, to the corresponding pair of internal states.

Interband transitions induced by the acceleration of the system, i.e., by the variation of the quasi-momentum, were studied in this (undriven) setting. Indeed, acceleration result-

ing from the effect of gravity was found to generate transitions which were satisfactorily described using the LZ model. The *activation* of gravity was arranged in practice by implementing the SOC in the vertical axis. Then, the trap was turned off, and the system was led to evolve under the effect of gravity. A qualitative understanding of the mechanism responsible for those interband transitions can be achieved from the analysis of Fig. 1(a) where the bands given by Eq. (3) are depicted. The curves  $E_{\pm}^{(ud)}(q)$  can be regarded as corresponding to the adiabatic levels (eigenvalues obtained for a *frozen* quasimomentum  $q$ ) of an effective LZ system. In this picture, the point of maximum proximity between the curves can be identified with the avoided crossing characteristic of the LZ model. In this framework, the inclusion of the acceleration, i.e., of varying  $q$ , implies going beyond that picture to take into account the potential occurrence of nonadiabatic effects, i.e., of interband transitions. The present work will be focused on analyzing how this scenario of LZ transitions is modified by the modulation of the Raman-coupling amplitude. Given the weakly-harmonic confinement realized in practice, a quasi-continuum approximation is feasible, and the use of the term “band” is still appropriate. When stronger harmonic confinement is considered, the description becomes more complex since the eigenstates of the Hamiltonian do not have a well-defined momentum (they are not eigenstates of  $P_y$ ). Actually, since the harmonic trapping alters the evolution of the momentum states, it can be regarded as an acceleration mechanism alternative to that associated to gravity.

### Transferring the modulation to multiple driving terms

The introduction of the modulation implies dealing with a time-dependent Hamiltonian. In our procedure to describe the dynamics, we start by applying the unitary transformation

$$U_1(t) = \exp \left[ -\frac{i}{2} \zeta(t) \hat{\sigma}_x \right], \quad (4)$$

where we have defined

$$\zeta(t) \equiv \eta_M \sin(\omega_M t), \quad (5)$$

with  $\eta_M = \Omega_M/\omega_M$ . The transformed Hamiltonian, obtained from the expression  $U_1^\dagger H_{SOC} U_1 - i\hbar U_1^\dagger \dot{U}_1$ , is written, after straightforward algebra, and, employing the same notation as that used for the untransformed Hamiltonian, in the form

$$H_{SOC}(t) = \left( \frac{\hbar^2 q^2}{2m} + E_r \right) \hat{1} + \frac{\hbar \Omega_0}{2} \hat{\sigma}_x + \left( \frac{\hbar \delta}{2} + \alpha q \right) [\hat{\sigma}_z \cos \zeta(t) + \hat{\sigma}_y \sin \zeta(t)]. \quad (6)$$

Emulating the experimental setup [22], where the detuning was adjusted to zero, we will take  $\delta = 0$ . The implications of a nonzero detuning will be discussed further on. Now, employing the expansion of  $\cos \zeta(t)$  and  $\sin \zeta(t)$  in terms of the ordinary Bessel functions  $J_n(\eta_M)$  [32],  $H_{SOC}(t)$  is rewritten as the sum of a basic undriven Hamiltonian and different oscillating contributions, namely,

$$H_{SOC}(t) = \left( \frac{\hbar^2 q^2}{2m} + E_r \right) \hat{1} + \frac{\hbar \Omega_0}{2} \hat{\sigma}_x + J_0(\eta_M) \alpha q \hat{\sigma}_z + 2J_1(\eta_M) \alpha q \hat{\sigma}_y \sin(\omega_M t) + \sum_{n>1} 2J_n(\eta_M) \alpha q \hat{\sigma}_i^{(n)} \cos(n\omega_M t), \quad (7)$$

where  $\hat{\sigma}_i^{(n)} = \hat{\sigma}_z$  when  $n$  is even, and  $\hat{\sigma}_i^{(n)} = \hat{\sigma}_y$  when  $n$  is odd.

The above expansion of the Hamiltonian was used in [28] to describe the dynamics in a former scenario of Raman-amplitude modulation [27]. Specifically, Eq. (7) was applied to set up a perturbative scheme that allowed the design of strategies to control the dynamics by varying the driving parameters. It is worth noticing that the strength of the modified zero-order term can be altered by varying the factor  $J_0(\eta_M)$  and the amplitude of the different oscillating contributions can be controlled by modifying  $J_1(\eta_M)$  and  $J_n(\eta_M)$  ( $n > 1$ ). The presence of those factors in reduced descriptions of systems with sinusoidal driving has been frequently used to design methods of control in different contexts [33]. The experimental results of [27] were satisfactorily explained using a model based on keeping the first driving term and neglecting, via a coarse-graining, the higher-order (oscillating) components (i.e., those with  $n > 1$ ) [28]. Actually, the applicability of the averaging method is justified for small modulation amplitudes and/or high frequencies: as  $\eta_M = \Omega_M/\omega_M$  decreases, the functions  $J_n(\eta_M)$  ( $n \geq 1$ ) decay and eventually go to zero. In the present work, we will keep on neglecting the contribution of those higher-order terms. However, in the analysis of the first oscillating component, we will go beyond the perturbative scheme used in [28].

### III. THE EFFECT OF THE MODULATION ON THE SPIN-MOMENTUM BANDS

#### Setting up an effective undriven framework

In [22], the dynamics of the modulated system was described applying the Floquet formalism. However, in order to operatively account for the experimental results, a functional *ad hoc* simplification of the Floquet framework was implemented: an effective time-independent two-level system with parameters adjusted to reproduce the experimental findings was employed. Here, we will apply an (alternative) approach based on a sequence of unitary transformations which will allow us to trace the applicability of an effective time-independent Hamiltonian from first principles. In order to simplify our procedure, we first rewrite the Hamiltonian given by Eq. (7), leaving out the terms with  $n > 1$ , as

$$H_{SOC}(t) = a(q)\hat{1} + b\hat{\sigma}_x + c(q)\hat{\sigma}_z + d(q)\hat{\sigma}_y \sin(\omega_M t), \quad (8)$$

where,

$$a(q) = \frac{\hbar^2 q^2}{2m} + E_r, \quad (9)$$

$$b = \frac{\hbar\Omega_0}{2}, \quad (10)$$

$$c(q) = J_0(\eta_M)\alpha q, \quad (11)$$

$$d(q) = 2J_1(\eta_M)\alpha q. \quad (12)$$

Moreover, using the function  $\beta(q)$  defined by

$$\beta(q) = \arctan \left[ \frac{b}{c(q)} \right], \quad (13)$$

Eq. (8) is recast as

$$H_{SOC}(t) = a(q)\hat{1} + \sqrt{b^2 + c(q)^2} [\hat{\sigma}_x \sin \beta(q) + \hat{\sigma}_z \cos \beta(q)] + d(q) \sin(\omega_M t)\hat{\sigma}_y, \quad (14)$$

Now, rotating an angle  $\beta(q)$  around the  $OY$  axis via the unitary transformation

$$U_2 = e^{-i\beta(q)\sigma_y/2}, \quad (15)$$



the Hamiltonian is converted into

$$U_2^\dagger H_{SOC} U_2 = a(q)\hat{1} + \sqrt{b^2 + c(q)^2}\hat{\sigma}_z + d(q)\sin(\omega_M t)\hat{\sigma}_y \equiv H_{SOC}(t). \quad (16)$$

Furthermore, in the rotating frame defined by

$$U_3(t) = e^{-i\omega_M t\sigma_z/2}, \quad (17)$$

one has

$$U_3^\dagger H_{SOC} U_3 - i\hbar U_3^\dagger \dot{U}_3 = a(q)\hat{1} + \left(\sqrt{b^2 + c(q)^2} - \hbar\omega_M/2\right)\hat{\sigma}_z + d(q)\sin(\omega_M t) [\cos(\omega_M t)\hat{\sigma}_y + \sin(\omega_M t)\hat{\sigma}_x] \equiv H_{SOC}(t). \quad (18)$$

Finally, making the Rotating Wave Approximation (RWA) [34], i.e., keeping the secular terms and neglecting oscillations of frequency  $2\omega_M$ , we arrive at

$$H_{SOC} = a(q)\hat{1} + e(q)\hat{\sigma}_z + \frac{d(q)}{2}\hat{\sigma}_x, \quad (19)$$

with

$$e(q) = \sqrt{b^2 + c(q)^2} - \hbar\omega_M/2. \quad (20)$$

Notice that the restriction  $|d(q)| \ll \omega_M$  must be fulfilled to guarantee the validity of the RWA. Observe also that the RWA is consistent with neglecting the higher-order oscillating terms in Eq. (7).

Hence, we have reached an effective time-independent Hamiltonian where the modulation of the Raman coupling amplitude has been included into the effective *parameters*  $e(q)$  and  $d(q)$ . Specifically, the splitting term  $e(q)$  incorporates the shift  $\hbar\omega_M/2$ , and, through  $c(q)$ , the driving-dependent factor  $J_0(\eta_M)$ ; furthermore, the coupling term  $\frac{d(q)}{2}$  absorbs the factor  $J_1(\eta_M)$ . Observe that both *parameters*  $e(q)$  and  $d(q)$  depend on the quasimomentum, i.e., the SOC enters two terms of the effective Hamiltonian. In the following, this framework will be shown to provide a valuable description of the system dynamics.

## Dressed states and modified spin-momentum locking

The eigenvalues of the Hamiltonian given by Eq. (19) are readily obtained:

$$E_{\pm}(q) = a(q) \pm \left[ e^2(q) + \frac{d^2(q)}{4} \right]^{1/2}. \quad (21)$$

Additionally, going back in the sequence of unitary transformations, the associated (dressed) eigenstates  $\{|\chi_{\pm}\rangle\}$  are expressed in the original basis  $\{|\downarrow\rangle, |\uparrow\rangle\}$  as

$$|\chi_{\pm}\rangle = F_{\pm,\uparrow}(t)|\uparrow\rangle + F_{\pm,\downarrow}(t)|\downarrow\rangle$$

where

$$\begin{aligned} F_{\pm,\uparrow}(t) = & C_{\pm,1}e^{i\omega_M t} \left( \cos \frac{\beta}{2} \cos \frac{\zeta}{2} - i \sin \frac{\beta}{2} \sin \frac{\zeta}{2} \right) + \\ & C_{\pm,2} \left( \sin \frac{\beta}{2} \cos \frac{\zeta}{2} + i \cos \frac{\beta}{2} \sin \frac{\zeta}{2} \right), \end{aligned} \quad (22)$$

and

$$F_{\pm,\downarrow}(t) = C_{\pm,1}e^{i\omega_M t} \left( -\sin \frac{\beta}{2} \cos \frac{\zeta}{2} + i \cos \frac{\beta}{2} \sin \frac{\zeta}{2} \right) + \quad (23)$$

$$C_{\pm,2} \left( \cos \frac{\beta}{2} \cos \frac{\zeta}{2} + i \sin \frac{\beta}{2} \sin \frac{\zeta}{2} \right), \quad (24)$$

with

$$C_{\pm,1} = \frac{d(q)/2}{\left( \frac{d^2(q)}{4} + [a(q) + e(q) - E_{\pm}]^2 \right)^{1/2}}, \quad (25)$$

and

$$C_{\pm,2} = -\frac{a(q) + e(q) - E_{\pm}}{\left( \frac{d^2(q)}{4} + [a(q) + e(q) - E_{\pm}]^2 \right)^{1/2}}, \quad (26)$$

In turn, the spin polarization in each of the bands is straightforwardly calculated, namely,

$$\langle \chi_{\pm} | \hat{\sigma}_z | \chi_{\pm} \rangle = |F_{\pm,\uparrow}(t)|^2 - |F_{\pm,\downarrow}(t)|^2. \quad (27)$$

Moreover, the averaging over the driving period  $T_M = 2\pi/\omega_M$  is directly carried out. In particular, for the averaged polarization along the lower band, one finds

$$\begin{aligned} \langle\langle \chi_- | \hat{\sigma}_z | \chi_- \rangle\rangle_{T_M} &= (|C_{-,1}|^2 - |C_{-,2}|^2) \cos \beta [J_0^2(\eta_M/2) - 2J_1^2(\eta_M/2)] + \\ &4C_{-,1}C_{-,2}J_0(\eta_M/2)J_1(\eta_M/2). \end{aligned} \quad (28)$$

From these results, some preliminary conclusions can be drawn:

i) The band structure is significantly altered by the modulation. The eigenvalues  $E_{\pm}(q)$ , depicted in Fig. 1(b), present significant differences with the undriven bands, contained in Fig. 1(a). Particularly conspicuous is the emergence of two-avoided crossings in the modulated system. This feature is specifically rooted in the driving: from Eq. (3), the difference between the undriven eigenvalues  $E_+^{(ud)}$  and  $E_-^{(ud)}$  is found to present a single minimum, reached at  $q = 0$ ; in contrast, in the modulated case, the difference between the energies  $E_{\pm}(q)$ , given by Eq. (21), display two minima, essentially because of the shift  $\hbar\omega_M/2$  in Eq. (20). Importantly, it is apparent that the separation between the avoided crossings increases with  $\omega_M$ . In the next section, the relevance of this property to extending the LZ model to deal with two avoided crossings will be apparent.

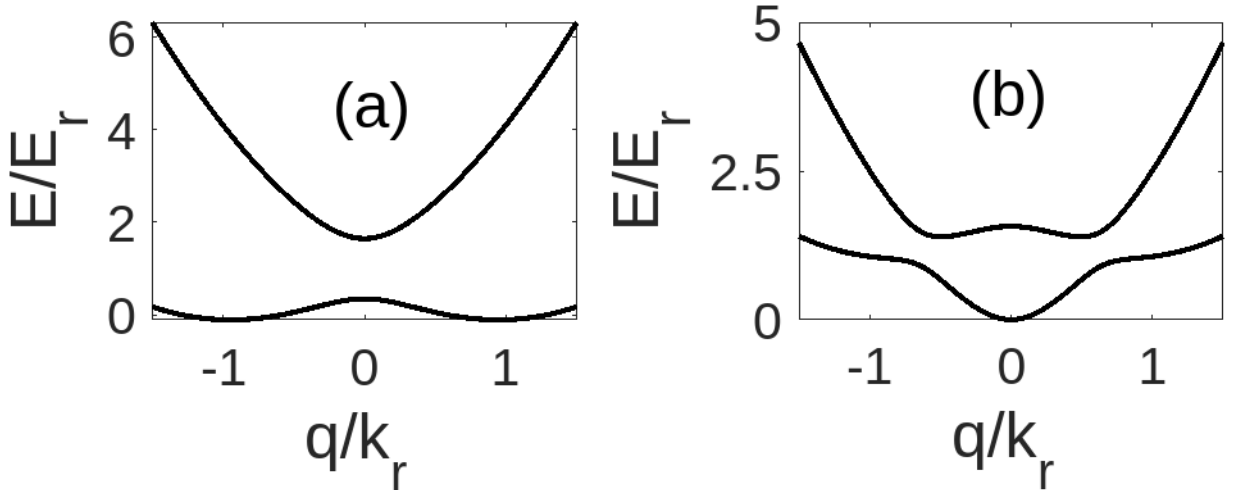


Figure 1: Energy-momentum dispersion relations for the unmodulated system (a) and for the modulated system (b) [In both cases,  $\Omega_0 = 1.3E_r/\hbar$ ,  $\delta = 0$ ; additionally,  $\Omega_M = 1.3E_r/\hbar$  and  $\omega_M = 2.87E_r/\hbar$  for (b)]. (In each case, the energy origin has been shifted to the lowest point in the first band).

ii) Additional information is extracted from the analysis of the dressed states. As can be seen in Fig. 2, where results for the polarization along the lower band are presented for the unmodulated state [Fig. 2(a)] and for the modulated (dressed) state [Fig. 2(b)], the driving of the Raman coupling amplitude alters significantly the distribution of population in the states  $\{|\downarrow\rangle, |\uparrow\rangle\}$ . The monotonous character of the evolution of the polarization in the undriven case disappears when the modulation is applied. The analytical character of our results allows choosing the modulation parameters to alter the polarization pattern. The experimental results presented in [22] are reproduced by our findings. No adjustable parameters have been employed. Observe that, whereas, in Fig. 2d in [22], the experimental results for the spin polarization are displayed as a function of time, our findings are presented as a function of the normalized quasimomentum.

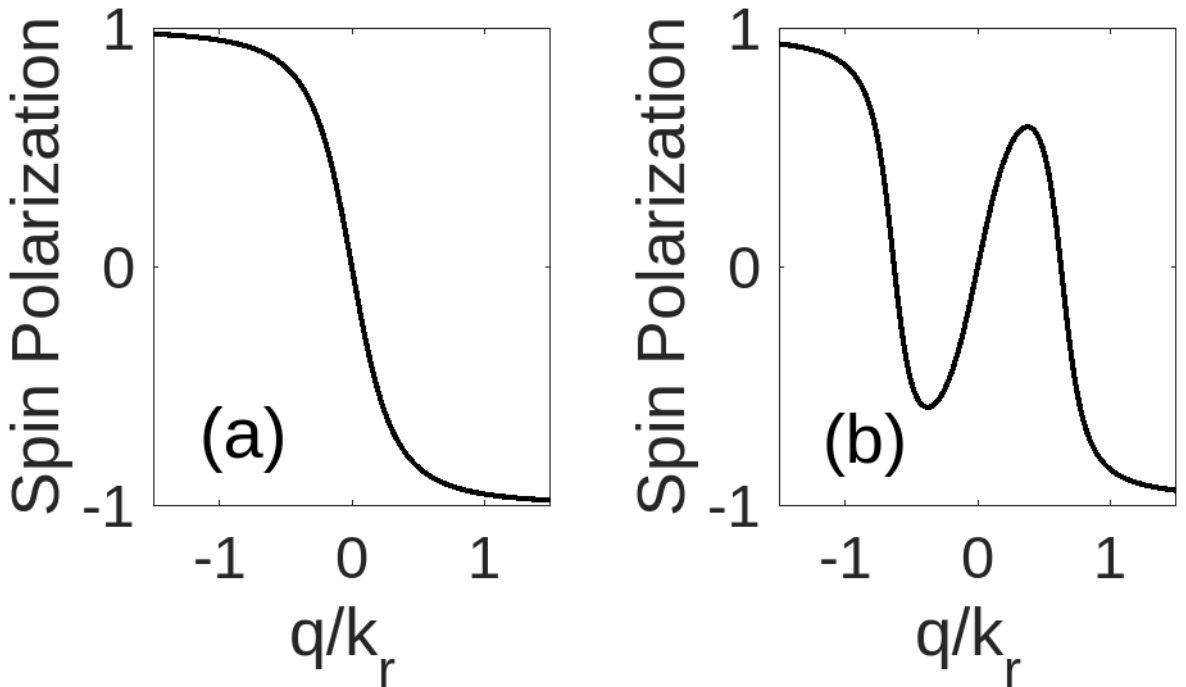


Figure 2: The spin polarization vs. the quasimomentum for the unmodulated system (a), and, for the modulated system (b). (Same parameters as in Fig. 1).

iii) Our results improve the effective two-level system operatively introduced in [22]. Two main contributions of our study must be remarked. First, our approach traces the presence of the driving-dependent factor  $J_0(\eta_M)$  in the splitting term  $e(q)$  of the model. Second, from our results, the effective coupling term is identified as  $\frac{d(q)}{2} = J_1(\frac{\Omega_M}{\omega_M})\alpha q$ . Here, it is worth recalling that the operative model of [22] incorporates an adjustable effective coupling

parameter, which was found to display a linear dependence on the modulation amplitude  $\Omega_M$ . That finding is confirmed and generalized by our study: the actual dependence of the effective coupling on  $\Omega_M$  is that included into  $J_1(\frac{\Omega_M}{\omega_M})$ . The linear dependence is specific to the range of amplitudes and modulation frequency considered in the experiment. Indeed, taking into account the approximation [32]

$$J_1\left(\frac{\Omega_M}{\omega_M}\right) \simeq \frac{1}{2} \frac{\Omega_M}{\omega_M} + \mathcal{O}\left[\left(\frac{\Omega_M}{\omega_M}\right)^3\right], \quad (29)$$

one accounts for the linear behavior found in [22]. This agreement is illustrated in Fig. 3, where the coupling parameter emergent in our model is represented as a function of  $\Omega_M$ . Notice that the range of  $\Omega_M/\omega_M$  where the decline of  $J_1(\frac{\Omega_M}{\omega_M})$  takes place is outside the regime explored in the experiments. Our results open the possibility of controlling the coupling by varying either  $\Omega_M$  or  $\omega_M$ .

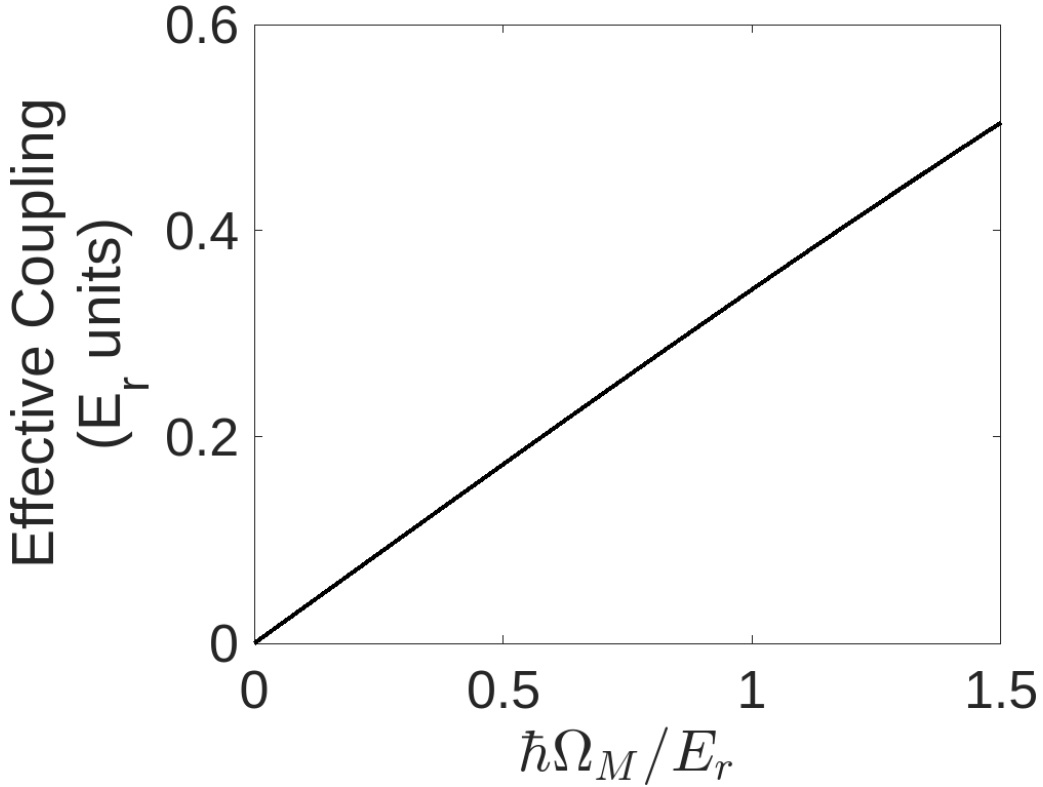


Figure 3: The effective-coupling term  $\frac{d(q)}{2} = J_1(\frac{\Omega_M}{\omega_M})\alpha q$  as a function of the modulation amplitude. ( $\Omega_0 = 1.3E_r/\hbar$ ,  $\delta = 0$ ,  $\omega_M = 2.87E_r/\hbar$ ,  $q = 1$ ).

iv) An additional feature uncovered by our results is the linear dependence of the effective

coupling term on both, the SOC strength  $\alpha$  and the quasimomentum  $q$ . In the next section, we will see the relevance of this finding to the understanding of the mechanism responsible for acceleration-induced transitions.

#### IV. LANDAU-ZENER TRANSITIONS INDUCED BY GRAVITATIONAL ACCELERATION

A significant achievement of the experiments of [27] was the uncovering of interband transitions induced by gravitational acceleration. In the practical arrangement, after implementing the SOC in the vertical axis, the trap was switched off and the system evolution under the effect of gravity was monitored. The changes in the band populations were tentatively explained using a LZ model with optimized characteristic parameters. Here, we will rigorously trace the emergence of that model.

According to the practical implementation, we consider that, at  $t = 0$ , the gravitational field is *activated*, the dynamics being then governed by the Hamiltonian

$$\begin{aligned} H_G &= H_{SOC} + H_{grav} \\ &= \frac{P_y^2}{2m} + E_r \hat{1} + \frac{\hbar \Omega_R(t)}{2} \hat{\sigma}_x + \frac{\alpha P_y}{\hbar} \hat{\sigma}_z + mgY, \end{aligned} \quad (30)$$

where, for  $H_{SOC}$  we have used the expression given by Eq. (1) with  $\delta = 0$ , and, the effect of the gravitational field has been assumed to be well modeled by the term  $H_{grav} = mgY$ . As shown in [35], this approach is convenient to operatively deal with the effects of gravity in the present context.

In the setup provided by Eq. (30),  $P_y$  is not a constant of the motion. The incorporation of gravity implies that the eigenstates of the Hamiltonian have no longer the form  $|p_y\rangle \otimes |\chi\rangle$ . In other terms,  $H_{grav}$  leads to the variation of the momentum in the evolution of a state  $|p_y\rangle \otimes |\chi\rangle$ , i.e., it induces the acceleration of the system.

Our procedure to deal with the dynamics resulting from the *incorporation* of gravity includes the consecutive application of two unitary transformation. The first one, given by

$$U_4(t) = \exp \left[ -\frac{i}{\hbar} mgYt \right], \quad (31)$$

introduces a time-dependent displacement in momentum: it implies working in a reference frame translated with acceleration  $g$ . The transformed Hamiltonian reads

$$U_4^\dagger H_G U_4 - i\hbar U_4^\dagger \dot{U}_4 = \frac{(P_y - mgt)^2}{2m} + E_r \hat{1} + \frac{\hbar\Omega_R(t)}{2} \hat{\sigma}_x + \frac{\alpha(P_y - mgt)}{\hbar} \hat{\sigma}_z \equiv H_G.$$

Further simplification is achieved by applying the transformation

$$U_5(t) = \exp \left[ -\frac{i}{\hbar} \left( \frac{P_y^2}{2m} + E_r \hat{1} \right) t + \frac{i}{\hbar} g P_y \frac{t^2}{2} \right], \quad (32)$$

which leads us to write the Hamiltonian in the form

$$U_5^\dagger H_G U_5 - i\hbar U_5^\dagger \dot{U}_5 = \frac{\hbar\Omega_R(t)}{2} \hat{\sigma}_x + \frac{\alpha(P_y - mgt)}{\hbar} \hat{\sigma}_z \equiv H_G, \quad (33)$$

where we have left out the dynamically irrelevant term  $\frac{1}{2}mg^2t^2$ , which simply shifts the energy origin by  $mg^2t^2/2$ . Now, working in the representation  $\{|p_y\rangle \otimes |\chi\rangle\}$ , the reduction to the spin space is readily implemented in the form

$$H_G = \frac{\hbar\Omega_R(t)}{2} \hat{\sigma}_x + \alpha q_g \hat{\sigma}_z, \quad (34)$$

with the *shifted* quasimomentum

$$q_g = \frac{p_y}{\hbar} - \frac{mg}{\hbar} t \equiv q - \frac{mg}{\hbar} t. \quad (35)$$

Finally, the application of a sequence of unitary transformations similar to those introduced in the previous section, i.e., the consecutive application of  $U_1$ ,  $U_2$ , and,  $U_3$ , leads to

$$H_G = e(q_g) \hat{\sigma}_z + \frac{d(q_g)}{2} \hat{\sigma}_x. \quad (36)$$

Here, it is worth pointing out that additional terms emerge when applying the transformation  $U_2(t) = e^{-i\beta(q_g)\sigma_y/2}$ , which is now time dependent because of the shift incorporated in  $q_g$ . Those terms are rooted in elements of the undriven dynamics as can be seen from the definition of  $\beta(q_g)$ . They are indeed relevant to recover the results obtained for the undriven scenario in [31]: they account for LZ transitions in the absence of driving. However, in the case considered here, where the modulation induces a significant modification of the energy bands, those terms can be considered to give a (nonsecular) correction to  $H_G$ . Hence, we keep them out of the description.

Let us see that it is possible to identify LZ characteristics in the dynamics resulting from Eq. (36). To this end, it is convenient to recall that the basic LZ model corresponds to a

two-level system described by the Hamiltonian

$$H_{LZ} = \hbar \frac{vt}{2} \hat{\sigma}_z + \hbar \zeta \hat{\sigma}_x, \quad (37)$$

where  $v$  stands for the variation rate of the energy mismatch, and  $\zeta$  denotes the interstate coupling strength. Whereas the diabatic states are the two (coupled) eigenstates of  $\sigma_z$ , the adiabatic states are the instantaneous eigenstates of the whole Hamiltonian  $H_{LZ}$ . At  $t = 0$ , there is a crossing of the diabatic levels which becomes an avoided crossing in the adiabatic picture.

From the comparison of the basic LZ scenario with our effective description of the modulated system, the following conclusions can be drawn:

i) By taking *frozen* values of the quasimomentum  $q_g$ , the adiabatic levels of the Hamiltonian given by Eq. (36) are readily obtained. They are depicted in Fig. 4(b). Notice that they are actually related to the dispersion curves (*dressed* bands) given by Eq. (21) and represented in Fig. 1(b). The differences are rooted in the terms removed via the application of the unitary transformation  $U_5(t)$  in the derivation of  $H_G$ . The acceleration leads to changes in the quasimomentum  $q_g$ , and, consequently, implies going beyond the adiabatic picture, accounting then for the occurrence of inter-band transitions.

ii) In the diabatic picture, the energy levels are the *bare* bands obtained by taking out the contribution of the off-diagonal term  $\frac{d(q_g)}{2} \hat{\sigma}_x$  in Eq. (36). Correspondingly, that term is now regarded as giving the coupling between the (diabatic) spin states. The diabatic levels are displayed in Fig. 4(a). This picture is appropriate to illustrate the identification of one of the characteristic parameters of the LZ model: the variation rate of the energy mismatch is obtained from the linearization of the diabatic levels at the crossings. One must stress that, in the primary LZ setup, it is the driving term,  $\hbar \frac{vt}{2} \sigma_z$ , independent of the considered dynamics, that induces the linear variation of the energy mismatch, and, eventually, the crossing. In contrast, in our system, it is the dynamics of the external variables, specifically, of the momentum, that leads to the modification of the internal-state splitting. In the applied reduction to the spin space, that dynamical effect takes the form of a driving component, namely, it turns into the form  $e(q - \frac{mg}{\hbar}t) \hat{\sigma}_z$ .



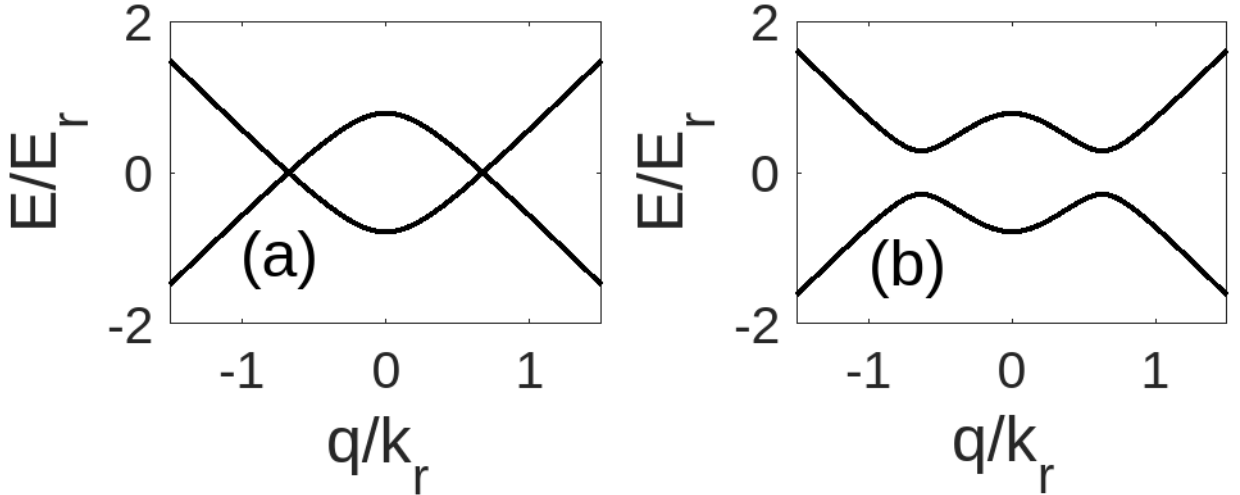


Figure 4: Diabatic (a) and adiabatic (b) energy-levels vs the quasimomentum for the effective LZ model. (Same parameters as for the modulated system in Fig. 1).

iii) An important differential feature of the present scenario is the existence of two avoided crossings, instead of just one as in the basic LZ model. Since the crossings are defined by the condition  $e(q_C) = 0$ , it follows from Eq. (20) that they are reached at the quasimomentum values

$$q_C = \pm \frac{\hbar}{2J_0(\eta_M)\alpha} \sqrt{\omega_M^2 - \Omega_0^2}. \quad (38)$$

The associated gaps in the adiabatic curves are determined by the effective *offset*  $d(q_C)$ : the adiabatic bands progressively separate as  $d(q_C)$  increases. Note that the condition  $\omega_M > \Omega_0$  must be fulfilled for a crossing to take place. Otherwise, the parallelism with the LZ model cannot be established.

iv) The identification of the effective parameters  $v_{eff}$  and  $\zeta_{eff}$  of the modulated system, (i.e., the counterparts of  $v$  and  $\zeta$  of the basic LZ model), is straightforward. In order to identify  $v_{eff}$ , the linearization of the energy mismatch at the level crossings is required. Specifically, one obtains that, near the crossing points, the time dependence of the energy splitting can be approximated as

$$e(t) \sim -\alpha \frac{mg}{\hbar} \frac{\sqrt{\omega_M^2 - \Omega_0^2}}{\omega_M} J_0(\eta_M)(t - t_C), \quad (39)$$

where  $t_C$ , which denotes the time at the crossing, depends on the initial momentum preparation. We do not need to specify the value taken by  $t_C$ : it is well-known from the study of

the LZ model [31] that the existence of an independent term in the linearly-modified energy mismatch does not affect the probability of transition

From the obtained rate of variation of the energy splitting at the crossing, one can establish the correspondence

$$|v_{eff}| \rightarrow \frac{2\alpha mg}{\hbar^2} \frac{\sqrt{\omega_M^2 - \Omega_0^2}}{\omega_M} J_0(\eta_M). \quad (40)$$

Apart from the *expected* dependence on  $g$ ,  $v_{eff}$  shows the relevance of the SOC strength  $\alpha$  and of the modulation frequency  $\omega_M$  to the rate of variation of the energy mismatch.

Additionally, the effective parameter  $\zeta_{eff}$  is traced from the value of the coupling term at the crossing:

$$\zeta_{eff} \rightarrow \frac{1}{\hbar} \frac{d(q_C)}{2} = \frac{J_1(\eta_M)}{2J_0(\eta_M)} \sqrt{\omega_M^2 - \Omega_0^2}. \quad (41)$$

It is pertinent to recall that the applied framework contains elements which are intrinsically associated to the modulation characteristics. Namely, the approach incorporates the condition  $\omega_M > \Omega_0$ , imposed to establish the parallelism with the LZ model. Additionally, it makes use of a reference frame rotating with  $\omega_M$ . Moreover, corrections associated to the transitions already present in the undriven system have been left out. Consequently, the present framework cannot account for the recovery of the results obtained for the unmodulated system [31].

v) In order to guarantee the applicability of the LZ expressions, the initial and final times of the process do not need to strictly correspond to  $t \rightarrow \mp\infty$ . The robust character of the LZ predictions imply that it is only necessary to work with sufficiently large values of the initial and final splittings. Observe that the separation between crossing points increase with the modulation frequency. Then, for sufficiently large values of  $\omega_M$ , one can assume that the *asymptotic* regime is reached between the crossings, and, consequently, that the LZ model can be safely applied to each of them. This is in fact the basis of Stueckelberg interferometry [26]. Let us make a more precise evaluation of the required magnitude of  $\omega_M$ . It is apparent that a sufficient condition for effectively reaching the asymptotic regime between crossings is to impose the duration of the LZ transition to be much smaller than the time taken for the parameter  $q_g(t)$  to go from one crossing to the other. This condition can be more precisely stated in the following form:

From basic work on the LZ model, it is known that the typical duration of the LZ transition  $\tau_{LZ}$ , i.e., the interval required for reaching the asymptotic population values, can be estimated as

$$\tau_{LZ} \sim \frac{\zeta_{eff}}{|v_{eff}|}.$$

Additionally, from our study, the quasimomentum separation between the two avoided crossings is shown to be given by

$$\frac{\hbar}{J_0(\eta_M)\alpha} \sqrt{\omega_M^2 - \Omega_0^2}.$$

In turn, the time  $\tau_{CC}$  taken for the variation of the parameter  $q_g(t)$  between crossings is given by

$$\tau_{CC} \sim \frac{\frac{\hbar}{J_0(\eta_M)\alpha} \sqrt{\omega_M^2 - \Omega_0^2}}{\frac{mg}{\hbar}}.$$

Hence, the condition required for having the avoided crossings sufficiently separated, and, consequently, for soundly applying the LZ model at each crossing is given by

$$\tau_{LZ} \ll \tau_{CC}.$$

Using the expressions of  $\tau_{LZ}$  and  $\tau_{CC}$  and taking  $J_0(\eta_M) \sim 1$  and  $J_1(\frac{\Omega_M}{\omega_M}) \sim \frac{\Omega_M}{\omega_M}$  for the magnitude of the Bessel functions, the above restriction is rewritten as

$$\Omega_M \ll \sqrt{\omega_M^2 - \Omega_0^2}$$

vi) The probability of transition between adiabatic states,  $P_{LZ}^{(a)}$ , is obtained by replacing, in the expression given by the standard LZ model [24, 25], the parameters  $v$  and  $\zeta$  by their counterparts in the present system,  $v_{eff}$  and  $\zeta_{eff}$ . Accordingly, we can write

$$P_{LZ}^{(a)} = e^{-2\pi|\zeta_{eff}|^2/v_{eff}}. \quad (42)$$

The validity of the whole approach, and, in particular, of this expression is confirmed by its applicability to the reproduction of the experimental results on interferometry.

vii) The effects of including a nonzero detuning  $\delta \neq 0$  in the SOC realization can be readily evaluated. The detuning is incorporated into our approach by replacing  $\alpha q$  by  $\frac{\hbar\delta}{2} + \alpha q$ . Consequently, the *parameter*  $c(q)$  is shifted as  $c(q) = J_0(\eta_M)(\alpha q + \frac{\hbar\delta}{2})$ . Also shifted

are the functions  $d(q)$  and  $e(q)$ . In order to analyze how those shifts affect the effective LZ parameters  $v_{eff}$  and  $\zeta_{eff}$ , the following remarks are pertinent. First, one must take into account that  $d(q)$  and  $e(q)$  incorporate the dependence on  $\delta$  through  $c(q)$ ; in particular,  $d(q)$  is proportional to  $c(q)$ . Second, the crossing, which is reached when  $e(q)$  takes a zero value, occurs at a value of the function  $c(q)$ , let us call it  $c(q_C)$ , which does not depend on  $\delta$ : as can be seen from Eq. (20),  $c(q_C)$  is merely determined by  $\omega_M$  and  $b$ . As a consequence, no dependence on  $\delta$  is apparent in  $d(q_C)$ , and, in turn, one can conclude that the coupling parameter of the LZ model  $\zeta_{eff} = \frac{1}{\hbar} \frac{d(q_C)}{2}$  is not affected by  $\delta$ . No changes are either observed in  $v_{eff}$ . Actually, a nonzero detuning simply alters the quasimomentum at the crossing  $q_C$ , and, consequently, leads to the appearance of a constant term in the linear variation of the energy mismatch, which does not modify the probability of transition.

## V. CONCLUDING REMARKS

The study provides a logical framework where the experimental results can be understood and the possibility of implementing controlled variations of the observed dynamics can be contemplated. The operativity of the study is rooted in the compact character of the model. Indeed, it is the robustness of the LZ scenario that allows the simplified presentation of the dynamics. Two examples are pertinent. First, since the activation of the transitions takes place only near the crossings, it is possible to cast the probability of transition into the standard LZ form by taking the coupling parameter at the quasimomentum value of the crossing point. Second, the applicability to the scenario with two avoided crossings is also associated to the soundness of the LZ model: the validity is guaranteed provided that the crossings are sufficiently separated for assuming that approximate *asymptotic-regime* conditions are reached between them.

By revealing the mechanisms responsible for the observed effects, the study provides us with predictive power on the feasibility of controlling diverse extensions of the setup. Particularly useful to the design of strategies of control is to have the precise functional form of the coupling term present in the emergent LZ model. Indeed, we have seen that it is the specific form of the coupling term that leads to the differential role of a nonzero detuning in the modulated system. Another interesting question that can be raised in connection with the coupling characteristics is the possibility of inhibiting the interband transitions by

appropriately choosing the modulation parameters. Specifically, given the form of  $d(q)$ , one can speculate on the feasibility of canceling the coupling by adjusting the amplitude  $\Omega_M$  and the frequency  $\omega_M$  of the applied sinusoidal driving in order to procure a zero of the factor  $J_1(\eta_M)$ . In fact, the analysis of that proposal cannot be made in the applied theoretical framework. In this sense, we must recall a crucial step in our procedure: the Hamiltonian with the multiple driving terms given by Eq. (7) was simplified using arguments relative to the magnitude of the ordinary Bessel functions. Namely,  $\eta_M$  was assumed to be small enough for allowing us to safely neglect the contributions of terms associated to Bessel functions of order higher than  $n = 1$ . Consequently, the realization of an argument  $\eta_M$  close to a zero of  $J_1(\eta_M)$ , which is outside the previously assumed working range, demands a reevaluation of the applied reduction. Actually, it is trivially shown that around the first zero of  $J_1(\eta_M)$ , different higher-order oscillating terms present contributions of similar magnitude. Hence, a simple reduction of the setup is not feasible.

Also important are the predictions allowed by our work on the potential use of different acceleration mechanisms. Since the transitions have been shown to be basically determined by the crossing-point properties, a system response with characteristics similar to those found in the study can be expected for alternative acceleration schemes. The case of a variation of the quasimomentum induced by a harmonic trapping must indeed be tackled in standard implementations. Although one can assume that the potential interband transitions can be described using a formalism similar to that used for gravitational acceleration, the analytical description of such scenario seems challenging given the nontrivial dynamics between transitions and the periodicity of the evolution. Correspondingly, the analysis of interferometry results when the harmonic-trap effects are important can be expected to be complex. Also interesting is to consider the potential applicability of the presented method to confinement in an accelerated optical lattice. Actually, the acceleration of an optical lattice implies including in the Hamiltonian a term completely analogous to the gravitational potential considered in the present study. However, from the periodic character of the lattice potential, which implies working with the Bloch-state representation, a variety of differential effects can be expected. Indeed, as  $\vec{P}$  is not a constant of the motion in the confined system, we conjecture that a much more complex treatment is needed to analyze the system dynamics in each period of the lattice.

Finally, a comment on the single-particle approach applied in the analysis is pertinent. In

[31], where the same atomic system was studied, a detailed analysis of nonlinear effects was presented. It was shown that, given the characteristics of the atomic-interaction strengths, it can be assumed that the many-body dynamics do not significantly modify the outcome of the single-approach picture. Specifically, the general predictions of the model were found to be robust when atomic-interaction effects were incorporated into the description. Those conclusions are in the line of the operative scheme used in the interpretation of the experimental work, where a single-particle approach was found to be sufficiently accurate to give a satisfactory understanding of the measurements. In this respect, it is also relevant to take into account the recent study presented in [36], where it is reported that a significant modification of the experimental conditions is required for making the interaction effects to be relevant to the performance of the LZ model.

- 
- [1] Y.-J. Lin, K. Jiménez-García, and I. B. Spielman, *Nature (London)* **471**, 83 (2011).
  - [2] Y. Zhang, G. Chen, and C. Zhang, *Sci. Rep.* **3**, 1937 (2013).
  - [3] ] D. L. Campbell, R. M. Price, A. Putra, A. Valdés-Curiel, D. Trypogeorgos, and I. B. Spielman, *Nat. Commun.* **7**, 10897 (2016).
  - [4] P. Wang, Z-Q. Yu, Z. Fu, J. Miao, L. Huang, S. Chai, H. Zhai, and J. Zhang, *Phys. Rev. Lett.* **109**, 095301 (2012).
  - [5] L. W. Cheuk, A. T. Sommer, Z. Hadzibabic, T. Yefsah, W. S. Bakr, and M. W. Zwierlein, *Phys. Rev. Lett.* **109**, 095302 (2012).
  - [6] Y. Li, G.I. Martone, and S. Stringari (2015) Spin-Orbit-coupled Bose-Einstein condensates. *Annual Review of Cold Atoms and Molecules*: pp. 201-250.
  - [7] Y. Chen, H. Lyu, Y. Xu, and Y. Zhang, *New J. Phys.* **24**, 073041 (2022).
  - [8] Tin-Lun Ho and Shizhong Zhang, *Phys. Rev. Lett.* **107**, 150403 (2011).
  - [9] Y. Li, L. P. Pitaevskii, and S. Stringari, *Phys. Rev. Lett.* **108**, 225301 (2012).
  - [10] Y. Li, G. I. Martone, L. P. Pitaevskii, and S. Stringari, *Phys. Rev. Lett.* **110**, 235302 (2013).
  - [11] J. Y. Zhang, S. C. Ji, Z. Chen, L. Zhang, Z. D. Du, B. Yan, G. S. Pan, B. Zhao, Y. J. Deng, H. Zhai, S. Chen, and J. W. Pan, *Phys. Rev. Lett.* **109**, 115301 (2012).
  - [12] Jin-Yi Zhang, Long Zhang, Zhi-Dong Du, Wei Zheng, You-Jin Deng, Hui Zhai, Shuai Chen, Jian-Wei Pan, *Nature Physics* **10**, 314 (2014).

- [13] Z. Chen and H. Zhai, *Phys. Rev. A* **86**, 041604(r) (2012).
- [14] T. Mithun, A. R. Fritsch, G. N. Koutsokostas, D. J. Frantzeskakis, I. B. Spielman, and P. G. Kevrekidis, *Phys. Rev. A* **109**, 023328 (2024).
- [15] T. Mithun and K. Kasamatsu, *Journal of Physics B: Atomic, Molecular and Optical Physics* **52**, 045301 (2019).
- [16] C. Hamner, Yongping Zhang, M. A. Khomehchi, Matthew J. Davis, and P. Engels, *Phys. Rev. Lett.* **114**, 070401 (2015).
- [17] Jun-Cheng Liang, Yan-Chao Zhang, Chen Jiao, Ai-Xia Zhang, and Ju-Kui Xue, *Phys. Rev. E* **103**, 022204 (2021).
- [18] Yi-Cai Zhang, Zeng-Qiang Yu, Tai Kai Ng, Shizhong Zhang, Lev Pitaevskii, and Sandro Stringari, *Phys. Rev. A* **94**, 033635 (2016).
- [19] N. Goldman, G. Juzeliunas, P. Ohberg, and I. B. Spielman, *Rep. Prog. Phys.* **77**, 126401 (2014).
- [20] A. Valdés-Curiel, D. Trypogeorgos, Q. Y. Liang, R. P. Anderson, and I. B. Spielman, *Nature Communications* **12**, 593 (2021).
- [21] J. Dalibard, F. Gerbier, G. Juzeliunas, and P. Ohberg, *Rev. Mod. Phys.* **83**, 1523 (2011).
- [22] A.J. Olson, D.B. Blasing, Chunlei Qu, Chuan-Hsun Li, R. J. Niffenegger, Chuanwei Zhang, and Yong P. Chen, *Phys. Rev. A* **95**, 043623 (2017).
- [23] A. Eckardt and E. Anisimovas, *New J. Phys.* **17**, 093039 (2015).
- [24] L. D. Landau, *Phys. Z. Sowjetunion* **2**, 46 (1932).
- [25] C. Zener, *Proc. R. Soc. A* **137**, 696 (1932).
- [26] S. N. Shevchenko, S. Ashhab, and F. Nori, *Phys. Rep.* **492**, 1 (2010).
- [27] K. Jiménez-García, L. J. LeBlanc, R. A. Williams, M. C. Beeler, C. Qu, M. Gong, C. Zhang, and I. B. Spielman, *Phys. Rev. Lett.* **114**, 125301 (2015).
- [28] J.M Gomez Llorente and J. Plata, *Phys. Rev. A* **93**, 063633 (2016).
- [29] A. J. Olson, Su-Ju Wang, R. J. Niffenegger, Chuan-Hsun Li, C. H. Greene, and Y. P. Chen, *Phys. Rev. A* **90**, 013616 (2014).
- [30] B. Xiong, J.H. Zheng, and D.W. Wang, *Phys. Rev. A* **91**, 063602 (2015).
- [31] J.M Gomez Llorente and J. Plata, *Phys. Rev. A* **94**, 053605 (2016).
- [32] I. S. Gradshteyn and I. M. Ryshik, *Table of Integrals, Series, and Products* (Academic Press, New York, 1994).

- [33] J.M Gomez Llorente and J. Plata, Phys. Rev. A **45**, R6958 (1992).
- [34] C. Cohen-Tannoudji, J. Dupont-Roc, and G. Grynberg, *Atom-Photon Interactions* (John Wiley & Sons, Inc., New York, 1992).
- [35] B. P. Anderson and M. A. Kasevich, Science **282**, 1686 (1998).
- [36] Zhiqian Gui, Jin Su, Hao Lyu, and Yongping Zhang, arXiv:2407.16109.